Switched flyback PFC converter for wide AC input voltage range

Yuki Kawai[1], Naoto Kikuchi[1], Hiroki Watanabe[1], Keisuke Kusaka[1], and Jun-ichi Itoh[1]

[1] Nagaoka University of Technology, Japan

Abstract— This paper proposes a switched flyback PFC converter for a universal input range applications. Conventional controllers have large number of components to realize the wide range voltage input, which reduces the efficiency. The proposed converter supports worldwide power supplies by two flyback converter and two additional switches. The proposed converter is based on two flyback converters and switches the connections of them in series or parallel according to the input voltage. Moreover, the proposed circuit is driven by the Triangular Current Mode (TCM) with variable frequency (VF) to achieve zero-voltage switching (ZVS). However, the VF causes the input current distortion because the input current is not proportional to the input voltage by changing the duty ratio. Therefore, this paper proposes the compensation method of the input current distortion using the TCM. The fundamental operation is demonstrated by the simulation and experiment. As the simulation result, it was confirmed that the input current distortion was improved by 99.2%. In the experimental result, the proposed circuit drives the power factor of 99.9 % by 1.0 p.u. in DCM operation.

Index Terms—**Flyback converter, Power Factor Correction, Wide range, Zero Voltage Switching.**

I. INTRODUCTION

Isolated AC/DC converters have been widely used as the switching power supply in many applications to obtain the DC voltage from single-phase or three-phase grid [1-5]. Power Factor Correction (PFC) techniques have been widely considered to compensate for the input current distortion to satisfy the IEC standard [6-8]. The two-stage configuration using the boost-type PFC converter is the common solution to obtain the sinusoidal input current [9-11]. However, additional magnetic components and switching devices are required for the PFC function, deteriorating the conversion efficiency [11,12]. In addition, the inductor in the boost circuit increases the volume of the converter. On the other hand, the single-stage PFC converter is also considered due to attractive advantages such as the simple configuration and the low number of components [13,14].

High power density and high-efficiency power conversion are also challenges for the isolated AC/DC converter with the universal input range [15-18]. The converters with the switching capability of the series/parallel connection have been proposed to extend the high-efficiency range with the various AC input voltage [19-23]. The parallel operation reduces current RMS and the conduction loss. On the other hand, the series operation reduces the voltage stress of switching devices. However, these converters require additional switching devices to change the series/parallel connections.

In order to solve the problem, the PFC converter based on the flyback converter has been proposed [11,24-26]. The flyback converter has advantages such as simple circuit configuration, low cost, galvanic isolation between input and output, and buck-boost operation capability. The flyback converter can improves the power factor of the input current without additional stages by operating with the Discontinuous Current Mode (DCM), which keeps the duty ratio and the switching frequency constant, to control the input current [27].

Zero Voltage Switching (ZVS) [28-30] using the Triangular Current Mode (TCM) and using the quasi-resonant method improve the efficiency of the flyback converter. The quasi-resonant method generates the resonant current to discharge the energy of the parasitic capacitance of the switching device during the dead-time period. On the other hand, in the TCM operation, the magnetizing current is controlled to the negative to discharge the parasitic capacitor. However, these ZVS methods are necessary to vary the switching frequency. As a result, the input current quality deteriorates because these methods do not meet the operating conditions for the PFC.

This paper proposes a switched flyback converter for the wide-range AC input voltage with the series/parallel connection. The proposed circuit consists of two flyback converters and a changeover circuit. The contribution of this paper is the realization of the high-power density and high efficiency in the wide range input voltage. Moreover, the control method is proposed to improve the input current quantity using the TCM operation by canceling the time variation of the duty ratio. As a result, the simulation results reveal that the proposed control method reduces the input current harmonics by 99.2 % compared to the conventional method. The validity of the proposed method is demonstrated by the simulation and experiment.

This paper is organized as follows. First, in section II, the circuit configuration of the proposed circuit is introduced and the operation is clarified. Next, in section III, the design of the controller and circuit parameters are described. In section IV, the validity of the proposed method is confirmed by the simulation. In section V, the proposed method is verified by the 240-W experimental prototype. Finally, the paper concludes in section VII.

II. CIRCUIT CONFIGURATION OF SWITCHED FLYBACK PFC CONVERTER

Figure 1 shows the circuit configuration of the proposed switched flyback converter. The proposed circuit consists of a synchronous rectifier and two active clamp flyback converters, and two additional switching devices for series

and parallel operation. The active clamp flyback converter has the capability of PFC, galvanic isolation, and DC voltage control for V_{dc}. The active clamp circuit which applies ZVS absorbs the surge voltage due to the leakage inductance of the high-frequency transformer. The proposed circuit adds two additional switching devices of S_6 and S_7 to realize the series and parallel operation.

The series and parallel operations are used depending on the input voltage variations. The series operation is applied under the high input AC voltage condition to divide the input voltage into two flyback converters. On the other hand, the parallel operation is used to share the large input current when low input AC voltage conditions.

III. OPERATION MODE

A. Series Operation

Figure 2 shows the operation mode of the proposed converter with a series connection. The proposed converter has two switching modes for the primary side of the flyback converter. The series operation composes the Input Series Output Parallel (ISOP) configuration. The universal input requires a high voltage and current rating for the power converter because the input specification is widely changed depending on the applications. Therefore, it is difficult to optimize the circuit design to realize the higher power density and efficiency when one converter is used.

The series operation based on ISOP is used for high input AC voltage conditions such as $300V_{rms}$ to $600V_{rms}$. The primary side of two flyback converters is connected in series to divide the input AC voltage. The secondary side of the flyback converter is connected in parallel to reduce the large current RMS in each converter because the secondary voltage is low as 24 V.

The series operation has two switching modes as shown in Fig. 2. Mode 1 starts when S_7 is turned on to charge the magnetic energy to the magnetizing inductance of two high-frequency transformers. Note that the magnetic energy is also charged to the leakage inductance L_{leak1} and L_{leak2}.

Mode 2 starts after mode 1 through the dead time. In this mode, the magnetic energy of the magnetizing inductance is transferred to the load when S_9 and S_{10} are turned on. In this mode, S_{11} and S_{12} are turned on to absorb the huge surge voltage in S_7 due to the leakage inductance. The active clamp circuit achieves ZVS to reduce the switching loss.

B. Parallel Operation

Figure 3 shows the operation mode of the proposed converter with a parallel connection. This operation also has two modes same as the series operation. The parallel operation composes the Input Parallel Output Parallel (IPOP) configuration to divide the input current. This operation is used for low input AC voltage conditions as 85 V_{rms}. Mode 3 starts when S_5 and S_8 are turned on to charge the magnetic energy to the magnetizing inductance. In this mode, each magnetizing inductance is connected in parallel. Finally, mode 4 starts after mode 3 through the dead time. This mode is for transferring the magnetic energy to the load same as mode 2.
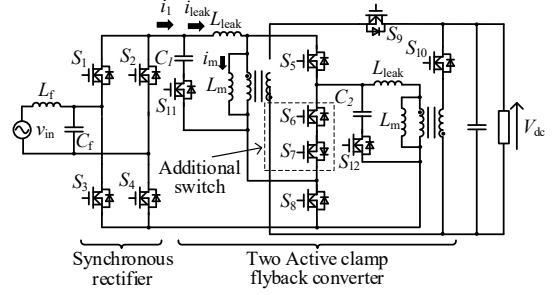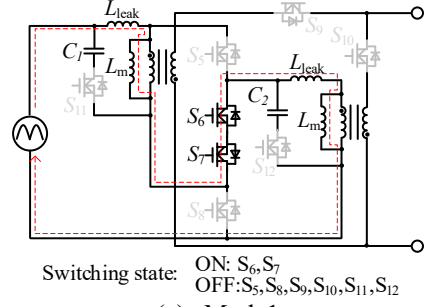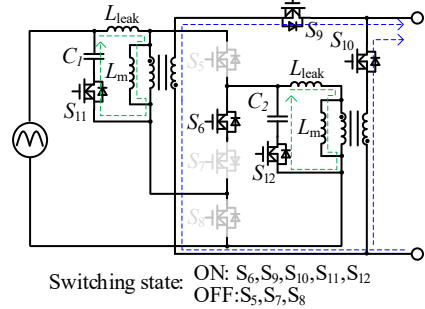

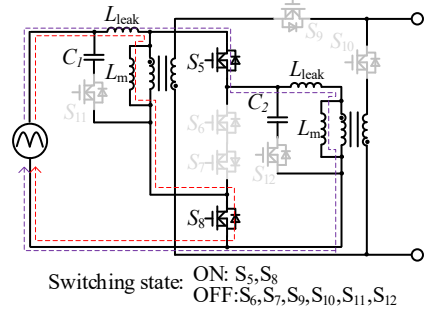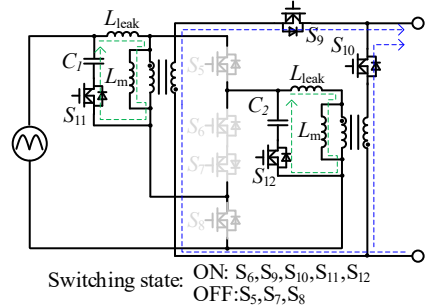Fig. 1. Circuit configuration of proposed converter.

Switching state: ON: S_6, S_7
OFF: S_5, S_8, S_9, S_{10}, S_{11}, S_{12}

(a) Mode1

Switching state: ON: S_6, S_9, S_{10}, S_{11}, S_{12}
OFF: S_5, S_7, S_8

(b) Mode2

Fig. 2. Switching state of series operation.

Switching state: ON: S_5, S_8
OFF: S_6, S_7, S_9, S_{10}, S_{11}, S_{12}

(a) Mode3

Switching state: ON: S_6, S_9, S_{10}, S_{11}, S_{12}
OFF: S_5, S_7, S_8

(b) Mode4

Fig. 3. Switching state of parallel operation.

IV. CONTROL METHOD

Figure 4 shows the magnetizing current waveform, switching state, and drain-source voltage of the flyback converter. The control method is implemented based on the Triangular Current Mode (TCM) to achieve ZVS for the flyback converter. The magnetizing current increases during mode 1 and mode 3 in each series and parallel operation. During the dead time, all switching devices are turned off. In this period, the parasitic capacitances of S_9, S_{10}, S_{11}, S_{12} are discharged by the magnetizing current. And then the magnetizing current decreases during mode 2 and mode 4 until the zero current. in TCM, the switching state of mode 2 and mode 4 continue during the delay period T_{delay} to make the negative current as shown in Fig.4. The parasitic capacitance of S_5, S_6, S_8, is discharged by the negative current during dead time. As the result, ZVS is achieved.

Figure 5 shows the control block diagram of the proposed control method. The TCM control is implemented based on the Boundary Current Mode (BCM) control. Firstly, the magnetizing current increases during the On-state period $T_{on}{}^*$. And then the magnetizing current decreases until zero current. In the case of the BCM control, the switching state is changed to $T_{on}{}^*$ when the zero current is detected. On the other hand, the TCM control continues the same switching state to generate the negative current. This switching state remains during the delay period $T_{delay}{}^*$.

The average of the primary current $i_{pri\_avg}(t)$ using the TCM is given by

$$i_{pri\_avg}(t) = \frac{|V_{in}\sin(\omega t)|}{2(L_m + L_{leak})}\frac{M(t)}{1+M(t)}T_{on} - I_{bot}\frac{M(t)}{1+M(t)} \quad (3)$$

$$M(t) = \frac{NV_{dc}}{|V_{in}\sin(\omega t)|} \quad\text{..}(4)$$

where V_{in} is the amplitude of the input voltage, V_{dc} is the output voltage, T_{on} is the actual On-state period, and M is the voltage ratio between primary and secondary side voltage, respectively. In the TCM control, the switching frequency varies depending on the grid voltage. In the case of the constant frequency modulation with the Discontinuous Current Mode (DCM), the sinusoidal input current is obtained when the constant duty ratio is applied. On the other hand, the input current in TCM is distorted due to the non-linear characteristics. Therefore, the linearization term $\alpha(t)$ is added to compensate for the input current distortion. $\alpha(t)$ is multiplied to the On-state command $T_{on}{}^*$ to eliminate the non-linear term in (3). The linearization term is given by

$$\alpha(t) = \frac{1+M(t)}{M(t)} \quad\text{..}(5)$$

On the other hand, the turn off time $T_{off}(t)$ for the secondary side switch of S_9 and S_{10} is given by

$$T_{off}(t) = \frac{L_{leak}}{L_m + L_{leak}}\frac{|V_{in}\sin(\omega t)|}{N(V_{dc}+V_f)}(T_{on}{}^* - T_d) \quad\text{...............}(6)$$

where T_d is the dead time, V_f is the forward voltage of the body diode in secondary switching devices. Besides, the period-to-period variation of I_{bot} is very small that it is assumed to be negligible.
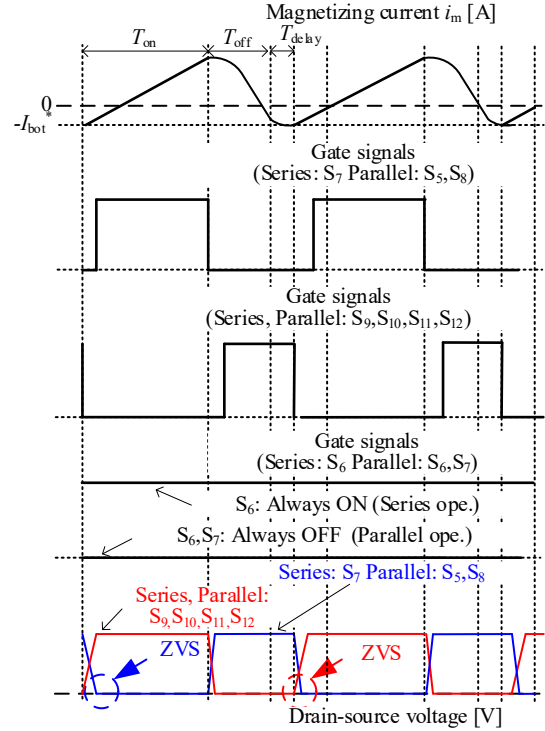

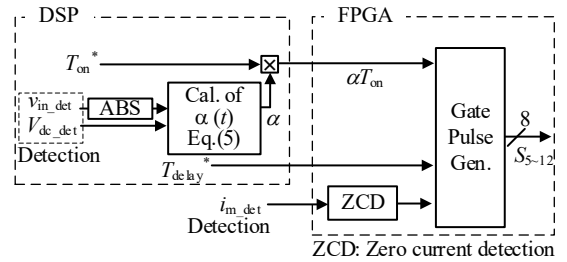Fig.4. Operation principle of transformer current and drain-source voltage.

Fig. 5. Control block diagram of proposed circuit.

Table. 1. Simulation parameters.

	Symbol	Value
Output power	P	240 W
Output DC voltage	V_{dc}	24 V
Input voltage	v_{in}	200,600 V_{rms}
Turn ratio	N:1	4:1
Magnetizing inductance	L_m	0.22 mH
Grid frequency	f	50 Hz

V. SIMULATION RESULT

Table 1 shows the simulation parameters. The input voltage is 600V_{rms} in the series operation, the input voltage is 200V_{rms} in the parallel operation, and the rated power is 240W. Note that the active clamp circuit and the input filter are not considered in this simulation.

Figure 6 shows the operation waveform compared with the conventional and proposed method in parallel operation. In the conventional method, the THD of the input current is 20.5%. On the other hand, in the proposed method, the THD is 0.17%.

Figure 7 shows the operation waveform compared with the conventional and proposed method in the series operation. In the conventional method, the THD of the input current is 24.3%. On the other hand, in the proposed method, the THD is 3.24%.

Figure 8 shows THD characteristics in the proposed circuit. As shown in figure 8, the input current THD of the series and parallel operation are drastically improved in wide output power condition. Especially, the input current THD of the parallel operation was improved to 20.1% from 1.57% when the output power is 0.1 p.u.. According to this result, it was confirmed that the input current THD was improved in wide output power condition by the proposed control.

VI. EXPERIMENTAL RESULT

Table 2 shows the experimental parameters. In this experiment, a series connection and a parallel connection are used at the input voltage 300V_{rms}, 150 V_{rms} respectively. Note that the diode rectifier and the capacitor are used instead of the synchronous rectifier.

Figure 9 shows the experimental results in the proposed circuit using DCM operation. Fig.(a) shows the experimental result of a series connection. Fig.8(b) shows the experimental result of a parallel connection. As the experimental result, the input power factor is 0.99 in a series connection and a parallel connection. In addition, the operation waveform of the primary current is generated during the zero-current period.
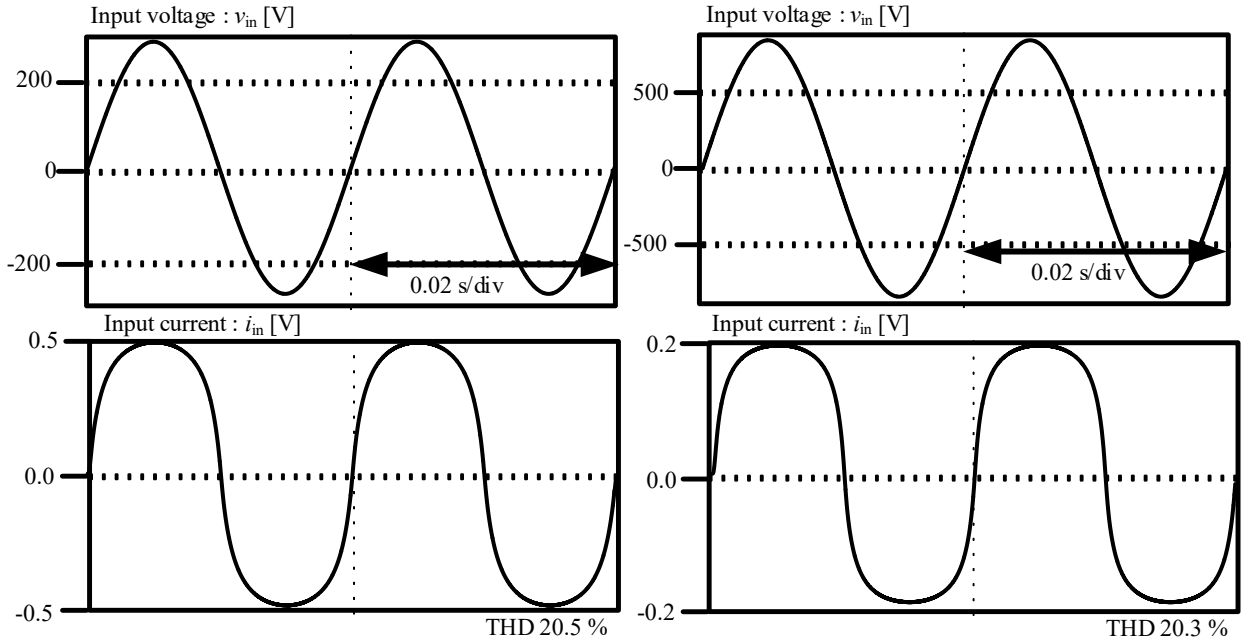
(a) Without proposed control

(b) With proposed control
Fig.6 Simulation result of parallel operation.
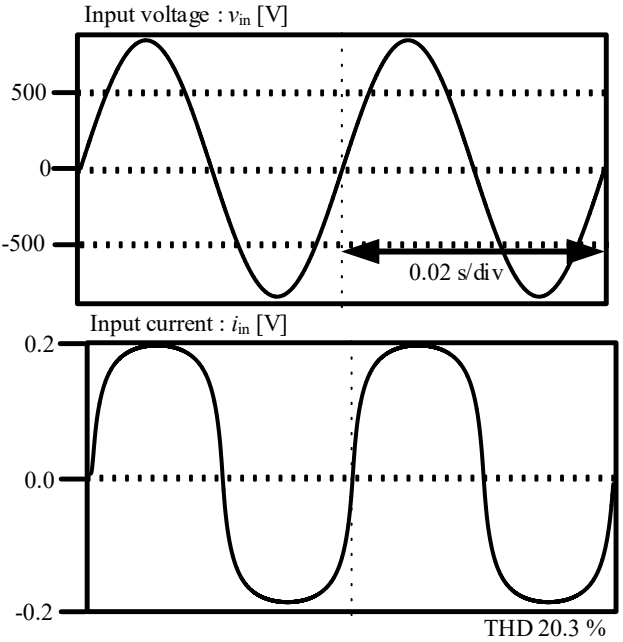
(a) Without proposed control

(b) With proposed control
Fig.7 Simulation result of series operation.

Figure 10 shows the THD characteristics in the proposed circuit. The flyback converter compensates for the harmonic component of the input current. However, in light load, THD of the input current exceeded 10% with both controls. Improving the THD is future work.

VII. CONCLUSION

This paper proposed the switched flyback PFC converter to realize the high-power density and high-power factor for a wide AC input voltage range. The proposed converter reduces component counts by sharing of switching devices of each converter. In addition, the proposed converter divides the voltage and current condition by the series and parallel connection. Furthermore, the ZVS method to ensure compatibility with PFC capability was proposed. The validity of the proposed method was demonstrated by simulation and experiment. As the simulation result, the input AC current THD was improved by 99.2 % when the proposed control was applied. As the experimental result, the validity of the proposed circuit is confirmed using the DCM operation. Thereby, the THD of the input current was 6.06 % in a series connection at 1.0p.u.. And, the THD of the input current was 1.54 % in a parallel connection at 1.0p.u..

In the future work, the validity of the proposed control with TCM will be considered in the experiment.

REFERENCES

[1] Lei Gu, et al.: A Wide-Input-Range High-Efficiency Step-Down Power Factor Correction Converter Using a Variable Frequency Multiplier Technique," in IEEE Trans on PE, Vol.33, No.11, pp. 9399-4214 (2018).

[2] Jingquan Chen, et al.: "Analysis and Design of a Low-Stress Buck-Boost Converter in Universal-Input PFC Applications," in IEEE Trans on PE, Vol.21, No.2, pp. 320-329 (2006)

[3] Yen-Ming Liu, et al.: " Single-Stage Soft-Switching AC/DC Converter With Input-Current Shaping for Universal Line Applications," in IEEE Trans on IE, Vol.56, No.2, pp. 467-479 (2009).

[4] Nie Hou, Yuzhou Li, Zhongyi Quan, Yun Wei Li, Andrew Zhou:"Unified Fast-Dynamic Direct-Current Control Scheme for Intermediary Inductive AC-Link Isolated DC-DC Converters" in IEEE Open Journal of Power Electronics, vol. 2, pp. 383-400(2021)

[5] Welton Da S. Lima, Luan Carlos Dos S. Mazza, Gustavo A. De L. Henn, Dalton De A. Honorio, Paulo P. Praca, Demercil De S. Oliveira, Jr. , Luiz Henrique S. C. Barreto : "A Bidirectional Isolated Integrated AC–DC Converter Based on an Interleaved 3-Level T-Type Power Converters" in IEEE Access, vol. 9, pp. 142754-142767(2021)

[6] Deliang WU, Madhura SONDHARANGALLA, and Rajapandian AYYANAR : "Isolated Bridgeless PFC Converter Based on Active-Clamped SEPIC" in CPSS Transactions on Power Electronics and Applications, vol. 7, no. 3, pp. 239-250(2022)

[7] Zhi Zhang, Junkai Wu, Liwei Meng, Zhaoyun Zhang, Xiao Tang, Bihua Hu, Wang Hu : "Analysis and Design of a Single-Stage Bridgeless Isolated AC-DC Resonant Converter for Programmable AC Power Source Applications" in IEEE Access, vol. 8, pp. 219071-219082(2020)
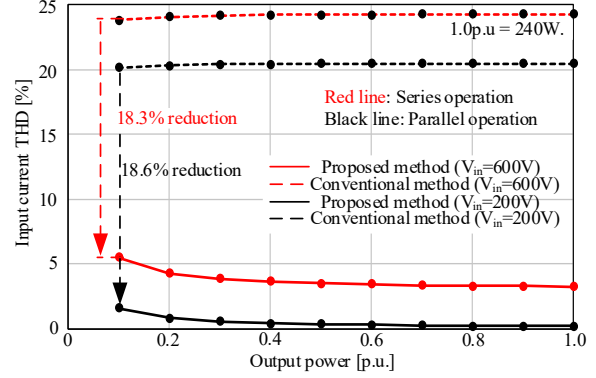
Fig. 8. THD characteristics compared with the conventional and proposed method.

Table. 2. Experimental parameters

	Symbol	Value
Output power	P	240 W(1.0 p.u)
Output DC voltage	V_{dc}	24 V
Input voltage	v_{in}	150, 300 V_{rms}
Turn ratio	N	4:1
Magnetizing inductance	L_{m1}	221.1 μF
Leakage inductance	L_{leak1}	9.1 μF
Magnetizing inductance	L_{m2}	223.18 μF
Leakage inductance	L_{leak2}	8.948 μF
Clamp capacitor	C_1	5 μF
Input capacitor	C_f	1 μF
Input inductor	L_f	2.2 mH
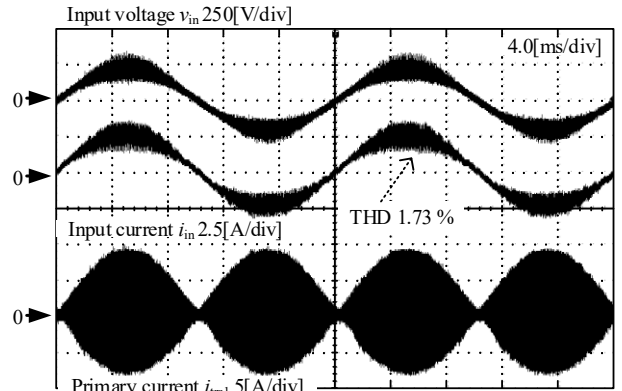
(a) Operation waveform in Parallel operation.
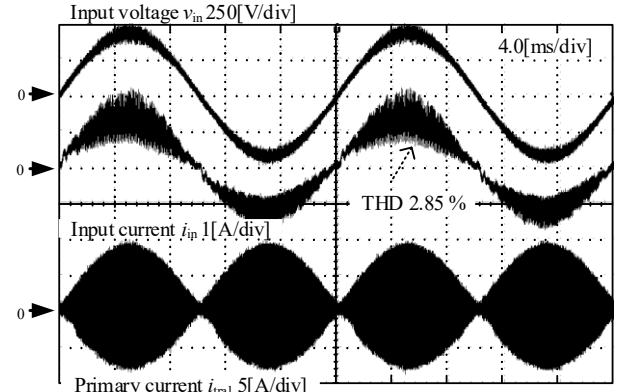
(b) Operation waveform in Series operation.

Fig. 9 Operation waveform using the DCM operation in the parallel and series operation.

[8] Qi Tian, Kevin(Hua) Bai : "Widen the Zero-Voltage-Switching Range and Secure Grid Power Quality for An EV Charger Using Variable-Switching-Frequency Single-Dual-Phase-Shift Control" in Chinese Journal of Electrical Engineering, vol. 4, no. 1, pp. 11-19(2018)

[9] G. Spiazzi and S. Buso, "An Isolated Soft-Switched High-Power-Factor Rectifier Based on the Asymmetrical Half-Bridge Flyback Converter," in IEEE Transactions on Industrial Electronics, vol. 69, no. 7, pp. 6722-6731(2022)

[10] B. Mahdavikhah and A. Prodić, "Low-Volume PFC Rectifier Based on Nonsymmetric Multilevel Boost Converter," in IEEE Transactions on Power Electronics, vol. 30, no. 3, pp. 1356-1372(2015)

[11] Y. -W. Kim, J. -H. Kim, R. -Y. Kim, B. -S. Suh and M. -G. Park, "A novel soft switched auxiliary resonant circuit of a PFC ZVT-PWM boost converter for an integrated power multi-chips module fabrication," 2012 IEEE Industry Applications Society Annual Meeting, Las Vegas, NV, USA, pp. 1-5 (2012)

[12] B. Singh, B. N. Singh, A. Chandra, K. Al-Haddad, A. Pandey and D. P. Kothari, "A review of single-phase improved power quality AC-DC converters," in IEEE Transactions on Industrial Electronics, vol. 50, no. 5, pp. 962-981(2003)

[13] A. K. Peter and J. Mathew, "A Single Phase, Single Stage AC-DC Multilevel LLC Resonant Converter With Power Factor Correction," in IEEE Access, vol. 9, pp. 70884-70895(2021)

[14] A. Tausif, H. Jung and S. Choi, "Single-stage isolated electrolytic capacitor-less ev onboard charger with power decoupling," in CPSS Transactions on Power Electronics and Applications, vol. 4, no. 1, pp. 30-39(2019)

[15] P. A. M. Bezerra, F. Krismer, R. M. Burkart and J. W. Kolar, "Bidirectional isolated non-resonant DAB DC-DC converter for ultra-wide input voltage range applications," 2014 International Power Electronics and Application Conference and Exposition, Shanghai, China, pp. 1038-1044 (2014)

[16] F. Canales, P. Barbosa and F. C. Lee, "A wide input voltage and load output variations fixed-frequency ZVS DC/DC LLC resonant converter for high-power applications," Conference Record of the 2002 IEEE Industry Applications Conference. 37th IAS Annual Meeting, Pittsburgh, PA, USA, pp. 2306-2313 vol.4 (2002)

[17] S. -J. Park, J. W. Park, K. H. Kim and F. -S. Kang, "Battery Energy Storage System With Interleaving Structure of Dual-Active-Bridge Converter and Non-Isolated DC-to-DC Converter With Wide Input and Output Voltage," in IEEE Access, vol. 10, pp. 127205-127224(2022)

[18] Hisashi Sekine, Hitoshi Haga, Yousuke Orii : "High-Efficiency Wide Range AC/DC Converter using Mode Transition of Six-Arm LLC" in IEEJ Journal of industry Applications, vol. 11, No. 5 pp. 696-708(2022)

[19] H. Hu, X. Fang, F. Chen, Z. J. Shen and I. Batarseh, "A Modified High-Efficiency LLC Converter With Two Transformers for Wide Input-Voltage Range Applications," in IEEE Transactions on Power Electronics, vol. 28, no. 4, pp. 1946-1960(2013)

[20] Y. Liu, H. Abu-Rub and B. Ge, "Front-End Isolated Quasi-Z-Source DC–DC Converter Modules in Series for High-Power Photovoltaic Systems—Part I: Configuration, Operation, and Evaluation," in IEEE Transactions on Industrial Electronics, vol. 64, no. 1, pp. 347-358(2017)

[21] J. Chen, K. Ding, Y. Zhong, F. Deng and S. Abulanwar, "A double input-parallel-output-series hybrid switched-capacitor boost converter," in Chinese Journal of Electrical Engineering, vol. 6, no. 4, pp. 15-27(2020)
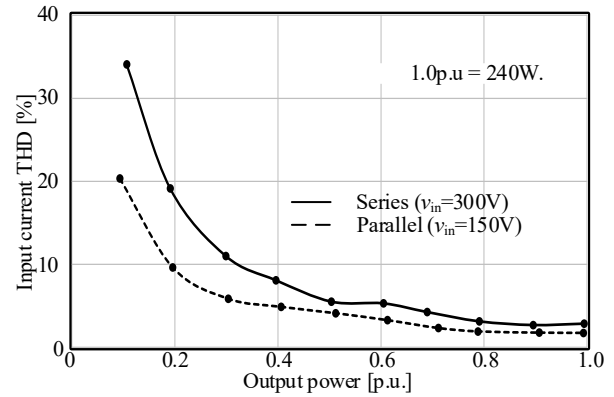
Fig. 10 THD characteristics in a parallel or series operation using DCM.

[22] Y. Li, S. Shao, H. Chen, J. Zhang and K. Sheng, "High-gain high-efficiency IPOS LLC converter with coupled transformer and current sharing capability," in CPSS Transactions on Power Electronics and Applications, vol. 5, no. 1, pp. 63-73(2020)

[23] Masahiro Sasaki, Koji Yano: "Turn On/Off Delay Time Control Balancing in Parallel Connected IGBTs without Increasing Switching Loss" in IEEJ Journal of industry Applications, vol. 11, No. 1 pp. 187-188(2021)

[24] D. Ð. Vračar, "Quasi-Resonant Flyback Converter as Auxiliary Power-Supply of an 800 V Inductive-Charging System for Electric Vehicles," in IEEE Access, vol. 10, pp. 109609-109625(2022)

[25] H. Luo, T. Zang, S. Chen and B. Zhou, "An Adaptive Off-Time Controlled DCM Flyback PFC Converter With Unity Power Factor and High Efficiency," in IEEE Access, vol. 9, pp. 22493-22502(2021)

[26] W. -T. Tsai, Y. -J. Chen and Y. -M. Chen, "A Modified Forward PFC Converter for LED Lighting Applications," in IEEE Open Journal of Power Electronics, vol. 3, pp. 787-797(2022)

[27] D. Gacio, J. M. Alonso, A. J. Calleja, J. Garcia and M. Rico-Secades, "A Universal-Input Single-Stage High-Power-Factor Power Supply for HB-LEDs Based on Integrated Buck-Flyback Converter," 2009 Twenty-Fourth Annual IEEE Applied Power Electronics Conference and Exposition, Washington, DC, USA, pp. 570-576(2009)

[28] G. Spiazzi, D. Tagliavia and S. Spampinato, "DC-DC flyback converters in the critical conduction mode: a re-examination," Conference Record of the 2000 IEEE Industry Applications Conference. Thirty-Fifth IAS Annual Meeting and World Conference on Industrial Applications of Electrical Energy, Italy, pp. 2426-2432 vol.4(2000)

[29] M. T. Zhang, M. M. Jovanovic and F. C. Y. Lee, "Design considerations and performance evaluations of synchronous rectification in flyback converters," in IEEE Transactions on Power Electronics, vol. 13, no. 3, pp. 538-546(1998)

[30] Y. Panov and M. M. Jovanovic, "Adaptive off-time control for variable-frequency, soft-switched flyback converter at light loads," in IEEE Transactions on Power Electronics, vol. 17, no. 4, pp. 596-603(2002)